Thoracic Cancer ISSN 1759-7706

ORIGINAL ARTICLE

Multi-slice computed tomography characteristics of solitary pulmonary ground-glass nodules: Differences between malignant and benign

Haiyang Hu[1†], Qingguo Wang[2†], Huamei Tang[3], Liwen Xiong[4*] & Qiang Lin[1*]

1 Department of Thoracic Surgery, Shanghai First People's Hospital, Shanghai, China
2 Department of Radiology, Shanghai First People's Hospital, Shanghai, China
3 Department of Pathology, Shanghai First People's Hospital, Shanghai, China
4 Department of Respiration, Shanghai Chest Hospital, Shanghai, China

Keywords
Multi-slice CT; pathology; persistent ground-glass nodule; three-dimensional reconstruction.

Correspondence
Liwen Xiong, Department of Respiration, Shanghai Chest Hospital, No. 241 West Huaihai Road, Shanghai 200030, China.
Tel: +86 21 63240090
Fax: +86 21 63240825
Email: hxxiongliwen@163.com

Qiang Lin, Department of Thoracic Surgery, Shanghai First People's Hospital, No. 100 Haining Road, Hongkou District, Shanghai 200080, China.
Tel: +86 21 36123603
Fax: +86 21 63240825
Email: xklinqiang@163.com

*Liwen Xiong and Qiang Lin contributed equally to this study as co-corresponding authors.
†Haiyang Hu and Qingguo Wang contributed equally to this study.

Received: 25 January 2015;
Accepted: 8 April 2015.

doi: 10.1111/1759-7714.12280

Thoracic Cancer **7** (2016) 80–87

Abstract

Background: Ground-glass nodules (GGNs), which are possible precursors of lung cancer, attract increasing attention. Many studies have attempted to identify the characteristic imaging features of GGNs for their qualitative diagnosis; however, the comprehension of GGNs remains controversial. We performed this study to identify imaging characteristics helpful to the differential diagnosis of solitary GGNs.

Methods: We retrospectively evaluated 112 solitary GGNs resected from 112 patients, pathologically examined after surgical resection. Imaging features of the GGNs, such as size, shape, a solid component, lobulation, spiculation, vascular convergence sign, pleural tag, and air cavity density, were assessed. Differences between malignant and benign nodules were analyzed using binary logistic regression analysis.

Results: Of the 112 GGNs, 82 were malignant and 30 were benign. A solid component, vascular convergence sign, and a larger diameter were risk factors for malignancy, with a sensitivity, specificity, and accuracy of 93.9%, 60.0%, and 84.8%, respectively. Lobulation, spiculation, air cavity densities, and pleural tags were also important indicators of malignancy, with positive predictive values of 93.5%, 83.3%, 91.7%, and 87.2%, respectively.

Conclusion: GGNs with a solid component, vascular convergence sign, and a larger diameter are highly suggestive of malignancy. The possibility of a neoplasm should also be considered in the case of GGNs that show lobulation, spiculation, air cavity densities, or pleural tags. To obtain a comprehensive and accurate analysis of the nodules, three-dimensional reconstruction is highly recommended.

Introduction

Lung cancer remains the leading cause of cancer death worldwide.[1] The five-year survival rate of patients with stage I–IV lung adenocarcinoma is merely 15%.[2] More than half of all patients with lung cancer will die within one year of diagnosis. However, if patients are diagnosed and treated at an early stage, the five-year survival rate can reach up to 50%.[3,4] As putative precursors of lung cancer, ground-glass nodules (GGNs) have attracted increasing research attention. The widespread use of computed tomography (CT) screening for early lung cancer detection has led to a remarkable increase in the detection of GGNs in the peripheral lung.[5,6]

Ground-glass nodules are areas of slightly and homogeneously increased density with preserved bronchial and vascular margins found on high-resolution CT, presenting differing characteristics in terms of shape, margins, and components.[7,8] Pathologically, these nodules may be caused by various disorders, such as partial airspace filling, interstitial thickening with inflammation, edema, fibrosis, neoplastic proliferation, and increased capillary blood volume.[9] As the differentiation of malignant from benign GGNs at

radiography is crucial for clinical diagnosis and management, many studies have attempted to identify the characteristic imaging findings of GGNs, proposing recommendations for the comprehension and management of the pulmonary nodules.[10–12] However, this endeavor is often hampered by the wide range of radiological manifestations of GGNs. There remains some controversy regarding which characteristics are valuable for the differential diagnosis of GGNs, such as the best frequency and duration of follow-up, and the best surgery method for resection. Development and complement of the comprehension of GGNs are also necessary. The aim of the present study was to retrospectively compare the features of pathologically proven malignant and benign solitary GGNs on thin-section CT images in an attempt to identify characteristics that would facilitate the differential diagnosis of solitary GGNs.

Methods

Subjects

We retrospectively reviewed solitary GGNs that were detected on screening or incidentally found, then surgically resected and pathologically confirmed at Shanghai First People's Hospital (Shanghai, China) between June 2012 and February 2015. GGNs that were found incidentally were included if there was no history of a pulmonary disease, chest trauma, or respiratory infection that could explain their presence. Bilateral or multiple nodules were excluded. Nodules that were still being followed up were excluded.

Approval for retrospective analyses and informed consent were not required according to our institutional guidelines.

Computed tomography imaging

All patients were scanned from the cupula of the pleura to the middle portion of the kidneys using a Light Speed VCT CT99 scanner (General Electric Medical Systems, Milwaukee, WI, USA). The scanning parameters were as follows: 120 kVp tube voltage; 100–120 mA tube current; and 512 × 512 pixel matrix size. All nodule imaging information was processed using Lung VCAR software (GE Healthcare Technologies, Milwaukee, WI, USA) on an AW Volume Share 2 workstation (GE Healthcare Technologies). Image reconstruction was performed with a 0.625 mm section thickness, a 0.984:1 pitch, and a 38.0 cm field of view, and the images were viewed in the mediastinal and pulmonary window settings. Three-dimensional (3D) reconstruction of the images was performed to display the morphology and margin characteristics, such as adjacent vessels. Two experienced radiologists who were blinded to the clinical data and histological diagnoses of the GGNs retrospectively assessed the CT scans. Decisions regarding the CT findings were reached by consensus.

The following CT features of the GGNs were assessed: nodule size, shape, margin characteristics, and internal characteristics. Nodule size was determined by measuring the maximal diameter. Nodule shape was classified as round/oval or irregular. Nodule margins were described as lobulated when a portion of the lesion's surface showed a wavy or scalloped configuration and as spiculated when strands extended from the nodule margin into the lung parenchyma. On the basis of the presence/absence of a solid component within the nodule on CT images in the lung window, we classified the nodules as part-solid GGNs or pure GGNs.[7] Part-solid GGNs had a solid component of soft-tissue density within the ground-glass component. For part-solid nodules, the size of the solid portion was measured by the maximal diameter. If crowding of internal vasculature or the presence of vessels abnormally angled toward the nodule, in comparison with the normal lung parenchyma, was determined, vascular convergence was considered to be present. A pleural tag was defined as a linear attenuation extending toward the pleura from a GGN. Air cavity densities included the vacuole sign and air bronchograms. The vacuole sign was defined as point-like, translucent, low-density shadows in the pulmonary nodules. An air bronchogram was defined as the direct involvement of a bronchiole in the nodules.

Pathological examination

The interval between pathological evaluation and the latest chest CT ranged from one to 35 days (mean, 7.8 days). All pathological specimens were obtained via open thoracotomy. The entire resected tissue specimen was fixed in formalin and embedded in paraffin. Several 4-μm-thick sections taken from the middle of the nodules were stained with hematoxylin-eosin and examined using light microscopy. Pathological diagnoses were based on 2004 World Health Organization criteria.[13] All tissue sections were interpreted by a pathologist with 27 years experience in lung pathology and confirmed by a more experienced pathologist. Of all the sections, adenocarcinomas were reevaluated according to the 2011 International Association for the Study of Lung Cancer/American Thoracic Society/European Respiratory Society international multidisciplinary classification of lung adenocarcinoma.[14]

Statistical analysis

Statistical analysis was carried out using SPSS version 18.0 (SPSS Inc., Chicago, IL, USA). Continuous data are presented as mean ± standard deviation, whereas categorical data are presented as numbers and percentages. Comparisons of different age and size groups were conducted using the *t*-test, while comparisons of gender and enumeration data were performed using the chi-square test. For variables with statistical significance, a logistic regression method was applied to make

a differential diagnosis between malignant and benign GGNs. Statistical significance was accepted at $P < 0.05$.

Results

In total, 112 nodules were analyzed in the present study. Of all GGNs included, 82 were diagnosed as malignant. Two nodules were diagnosed as adenosquamous carcinoma, four as adenocarcinoma in situ (AIS), nine as minimally invasive adenocarcinoma (MIA), and 67 as invasive adenocarcinoma, comprising of lepidic predominant ($n = 35$), acinar predominant ($n = 19$), papillary predominant ($n = 5$), micropapillary predominant ($n = 7$) and solid predominant with mucin production ($n = 1$). The remaining 30 were diagnosed as benign, and were comprised of inflammation ($n = 22$), atypical adenomatous hyperplasia ($n = 7$), and focal fibrosis ($n = 1$). Univariate analysis of the demographic data and selected CT features of the GGNs is shown in Table 1.

Comparison between malignant and benign ground-glass nodules

In our study, the nodule data was from 36 men and 76 women, aged 37–79 years. Malignant and benign GGNs did not significantly differ in terms of gender (54 women/28 men vs. 22 women/8 men, respectively; $P = 0.453$) or age (55.5 ± 9.3 years, range: 37–79 years vs. 52.5 ± 6.7 years, range: 38–67 years, respectively; $P = 0.106$). Malignant GGNs were significantly larger (average diameter, 14.6 ± 6.7 mm) than benign GGNs (average diameter, 9.3 ± 4.0 mm; $P < 0.001$). Of the 82 malignant nodules, 76 were part-solid GGNs, and six were pure GGNs. Of the 30 benign nodules, 12 were part-solid GGNs, and 18 were pure GGNs. Chi-square testing revealed that a central solid component (part-solid GGNs) was associated with malignancy ($P = 0.000$). For part-solid GGNs, the size of solid portion was significantly larger in malignant nodules (9.7 ± 4.7 mm) than in benign nodules (6.9 ± 2.9 mm; $P = 0.012$).

With respect to other morphological features of GGNs, we found significant differences between malignant and benign GGNs in terms of the incidence of lobulation (52.4% vs. 10.0%, $P = 0.000$; Figs 1, 3), air cavity densities (53.7% vs. 13.3%, $P = 0.000$; Fig. 1), vascular convergence sign (84.1% vs. 40.0%, $P = 0.000$; Figs 2, 3), pleural tags (41.5% vs. 16.7%, $P = 0.015$; Fig. 3), and spiculation (61.0% vs. 33.3%, $P = 0.009$; Fig. 3). Statistically significant differences were not found between malignant and benign GGNs with regard to nodule shape (round/oval vs. irregular; $P = 0.111$).

Table 1 Univariate analysis of demographic data and selected CT features of GGNs

	Malignant ($n = 82$)	Benign ($n = 30$)	*P*-value
Age (years)	55.5 ± 9.3	52.5 ± 6.7	0.106[a]
Size (mm)	14.6 ± 6.7	9.3 ± 4.0	0.000[a]
Gender ratio			
Male	28	8	0.453[b]
Female	54	22	
Shape			
Round/oval	44	11	0.111[b]
Irregular	38	19	
Solid component			
Yes	76	12	0.000[b]
No	6	18	
Lobulation			
Yes	43	3	0.000[b]
No	39	27	
Spiculation			
Yes	50	10	0.009[b]
No	32	20	
Vascular convergence			
Yes	69	12	0.000[b]
No	13	18	
Pleural tag			
Yes	34	5	0.015[b]
No	48	25	
Air cavity density			
Yes	44	4	0.000[b]
No	38	26	

[a]*t* test. [b]chi-square test. CT, computed tomography; GGNs, ground-glass nodules.

Binary logistic regression analysis

In binary logistic regression analysis, malignancy and benignity were included as induced variables, and solid component, lobulation, spiculation, vascular convergence, pleural tags, air cavity densities, and nodule size were regarded as covariates. The results of the analysis showed that solid component, vascular convergence sign, and a larger diameter were important indicators of malignancy in GGNs. The following regression equation was obtained using multiple regression analysis: $\ln(p/1\text{-}p) = -3.156 + 2.463 \times \textit{solid component} + 1.628 \times \textit{vascular convergence} + 0.116 \times \textit{nodule diameter}$ (Table 2), where "p" is the probability of malignancy. The risk of malignancy for a solitary GGN with a solid component and vascular convergence was 11.745-fold and 5.095-fold that of a GGN without these characteristics, respectively. As the nodule diameter increased by 1 mm, the risk of malignancy increased 1.123-fold. The sensitivity, specificity, and accuracy obtained with the regression equation were 93.9%, 60.0%, and 84.8%, respectively (Table 2).

Discussion

The findings of our study determined that the presence of a solid component, lobulation, vascular convergence sign, or an air cavity density were predictive of malignancy, while the absence of spiculation and pleural tag were associated with benignity.

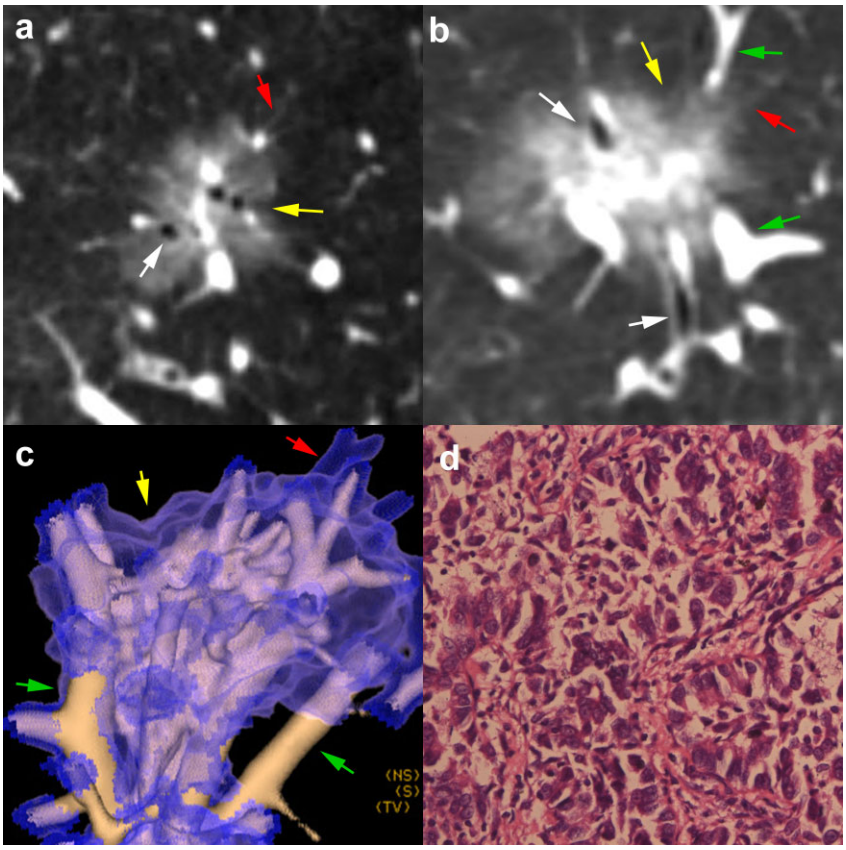

Figure 1 Nodule in the right upper lobe of a 52-year-old man. Computed tomography (CT) shows signs of lobulation (yellow arrow, **a/b**), vacuole sign (white arrow, **a**), vascular convergence (green arrow, **b**), slight spiculation (red arrow, **a/b**), and bronchus cut-off (white arrow, **b**). Three-dimensional reconstruction clearly displays the solid portion (central white part, **c**) and ground-glass density (blue part, **c**). Lobulation (yellow arrow, **c**), spiculation (red arrow, **c**), and vessels (green arrow, **c**) are also well constructed. (**d**) The nodule was pathologically diagnosed as adenocarcinoma.

Nodule size

Nodule size was a good indicator of the probability of malignancy. The possibility of malignancy gradually increased with increasing nodule diameter. The rate of malignancy among GGNs with a diameter ≤10 mm was 56.0% (28/50), while among nodules >10 mm, the malignancy rate was 88.7% (55/62). Our results are consistent with a previous study, which reported that 47.4% of pulmonary nodules measuring <10 mm were malignant, while 70.1% of nodules measuring >10 mm were malignant.[15] This suggests a close correlation between nodule size and malignancy. Several other studies have also demonstrated that smaller nodules are associated with benignity, while larger nodules tend to be malignant.[16,17] Wahidi *et al*. estimated that the prevalence of malignancy was <1% in nodules measuring <5 mm and >80% in those measuring >20 mm.[5] In the present study, no pure GGNs ≤5 mm were found to be malignant; this is in accordance with the Fleischner Society guidelines, which state that no CT follow-up is required for solitary pure GGNs measuring ≤5 mm.[18] However, four part-solid nodules with a diameter ≤5 mm were found to be malignant in the present study. Cases of malignant nodules <5 mm have also been reported.[19] Thus, malignant nodules cannot be differentiated from benign nodules on the basis of size alone. Although the Fleischner Society guidelines accept a 5 mm diameter threshold initially proposed by the Early Lung Cancer Action Project, great efforts should be taken to formulate a more detailed and accurate size criterion for the discrimination of malignant and benign nodules.[20]

Solid component

In part-solid GGNs, the solid portion may represent alveolar collapse, fibrosis, intra-alveolar mucus, or invasive carcinoma.[21] Malignancy was much more likely if a solid component was present and the probability of nodule malignancy increased with the size of the solid portion. The positive predictive value (PPV) of this characteristic was 86.4% (76 of 88 part-solid GGNs were malignant). In contrast, only 25.0% (6/24) of pure GGNs were confirmed to be malignant. Nakata *et al*. reported that 93% of persistent GGNs that contained a

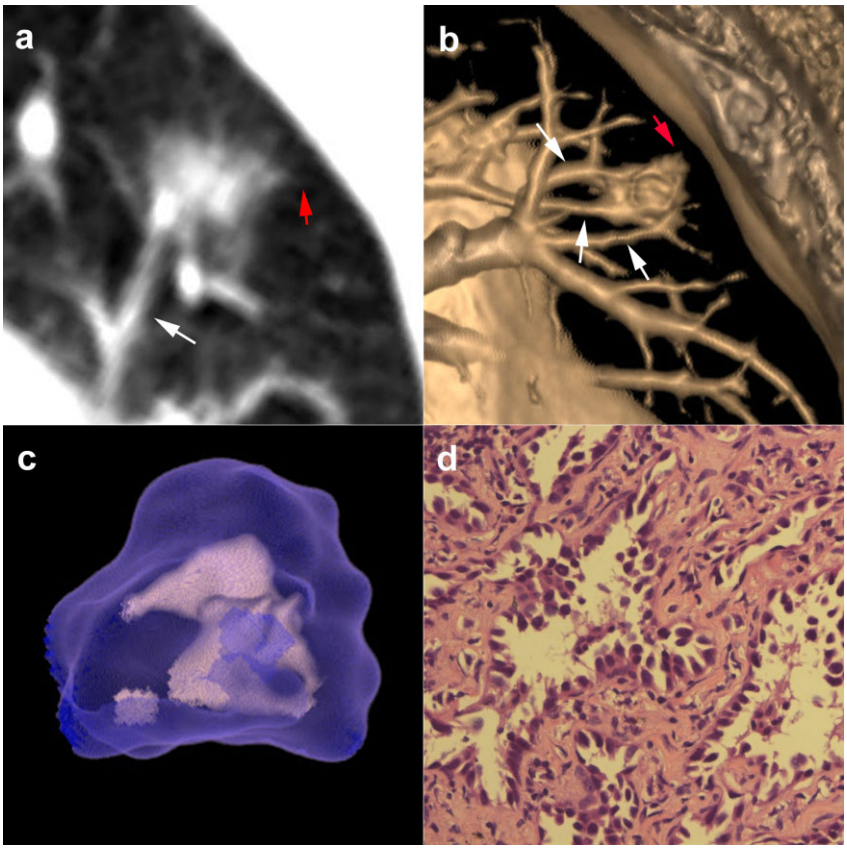

Figure 2 Nodule in the right upper lobe of a 57-year-old woman. Computed tomography (CT) shows vascular convergence sign (white arrow, **a**) and slight spiculation (red arrow, **a**). The vessels are entirely reconstructed by three-dimensional reconstruction and it is clearly visualized that the vessels converge on the nodule (white arrow, **b**). The morphology, solid portion (white part), and ground-glass density (blue part) can also clearly be seen by three-dimensional reconstruction (**c**). (**d**) The nodule was pathologically diagnosed as adenocarcinoma.

solid component were identified to be neoplasms in their study.[16] Similarly, Henschke *et al*. reported a malignancy rate of 63% in partially solid nodules and 18% in pure GGNs.[22] In the series reported by Li *et al*., part-solid GGNs were associated with malignancy in 85% of cases.[10] Thus, we strongly recommend that part-solid GGNs be meticulously evaluated.

Vascular convergence sign

The vascular convergence sign is a crucial indicator of malignancy. Angiogenesis is essential for tumor growth and metastasis.[23,24] As vascular endothelial growth factor is synthesized continuously and excessively in tumors, vascular endothelial cells proliferate during vessel formation and tumor vessels remain immature.[24,25] The immature tumor vessels are highly permeable, which causes the edema of the tumor tissue.[24] This may explain the ground-glass density of the nodule.[9] In our studied sample, the vessels did not adjoin or contact the edge of the nodule but rather converged on the nodule. The malignancy rate of GGNs with the vascular convergence sign was high (85.2%, 69/81), though this sign was also observed in 40.0% (12/30) of benign nodules. Our findings are consistent with the results of Mori *et al*. and Kuriyama *et al*. who reported that the involvement of pulmonary veins within GGNs strongly suggests malignancy.[26–27]

Three-dimensional reconstruction

We highly recommend 3D reconstruction of GGN images to enable accurate evaluation of the nodules. Lung VCAR software can automatically analyze whether a nodule is pure ground-glass, part-solid, or solid. It is not easy to identify a vertical bronchus or a vertical vessel on a cross-sectional CT scan, as these structures present with variable dimensions. The 3D reconstruction of nodules can overcome this disadvantage without increasing the amount of radiation. As the software automatically calculates the adjacent relationship of the nodule to marginal structures and 3D reconstructed images display nodules from different angles, it is possible to

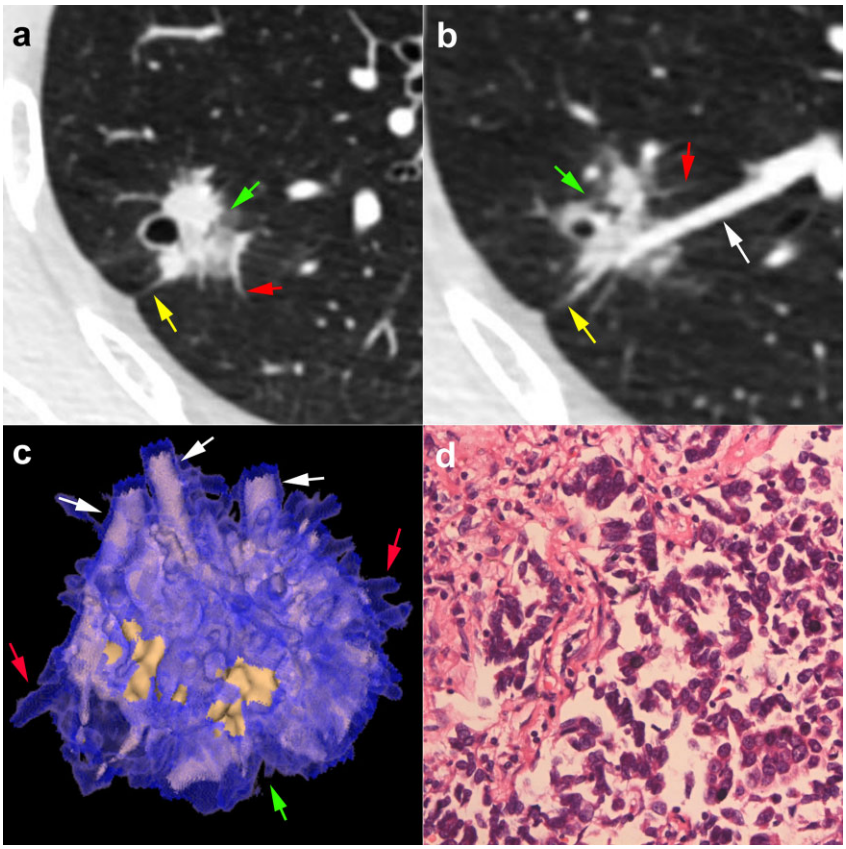

Figure 3 Nodule in the right upper lobe of a 51-year-old man. Computed tomography (CT) shows spiculation (red arrow, **a/b**), pleural tag (yellow arrow, **a/b**), lobulation (green arrow, **a/b**), and vascular convergence sign (white arrow, **b**), which is clearly displayed by three-dimensional reconstruction (**c**). (**d**) The nodule was pathologically diagnosed as adenocarcinoma.

clearly and accurately assess the anatomical morphology and margin characteristics, especially the vascular morphology and changes in the pleura and bronchi. Different components of the nodule are displayed with different colors so that the solid component is also displayed clearly. During the follow-up period, the solid portion of the nodule, changes of morphology, and nodule size could be objectively evaluated by the software without interference from human factors. Thus, 3D reconstruction enables a comprehensive analysis of the nodule, benefits the location and qualitative diagnosis of GGNs, and facilitates surgical planning. As shown in Figures 2 and 3, vessels converging on the nodules can be entirely reconstructed and visualized clearly on 3D reconstructed images, suggesting that compared with benign nodules, the demand for blood supply to enable cell proliferation is high in neoplastic nodules.

Table 2 Binary logistic regression analysis of CT characteristics of GGNs

	Variables in the equation							
Independent variables and constant	B	SE	Wals	df	Sig	Exp(B)	Exp(B) 95% CI Lower	Exp(B) 95% CI Upper
Solid component	2.463	o.624	15.577	1	0.000	11.745	3.456	39.914
Vascular convergence	1.628	0.577	7.973	1	0.005	5.095	1.646	15.777
Nodule diameter	0.116	0.059	3.799	1	0.051	1.123	0.999	1.262
Constant	–3.156	0.873	13.080	1	0.000	0.043		

B, regression coefficient; CI, confidence interval; CT, computed tomography; df, degrees of freedom; Exp(B), e^B = odds ratio; GGNs, ground-glass nodules; SE, standard error; Sig, significance; Wals, chi-square value.

Air cavity density

An air cavity density is defined as a round or branched air attenuation in the nodule. This sign is significant for the diagnosis of GGNs. In adenocarcinomas, air cavity densities represent lepidic tumor growth along pulmonary structures and bronchi.[28] An air bronchogram may be slightly distorted or dilated. This is visualized particularly when retractile fibrodesmoplastic reaction is present within the tumor. In the present research, air cavity densities were more frequent in neoplastic peripheral GGNs than in non-neoplastic peripheral GGNs. The PPV was 91.7% (44/48). Several other series have also revealed that the presence of air bronchograms and the vacuole sign is suggestive of adenocarcinoma.[28–31] However, another study found that air bronchograms were present in approximately 50% of old inflammatory nodules.[32] The small sample size in the study (18 nodules included) may explain this difference in malignancy rates.

Margin characteristics

Margin characteristics also contributed to the differentiation between malignant and benign nodules. Spicules and lobulated margins represent irregular interstitial fibrosis and imply an area of more rapid growth within a nodule.[12,33] The pathological basis of malignant lobulation is the difference in the growth velocity of various cells. The adjacent pulmonary interstitium blocks tumor growth, and the fibrous tissue inside the nodule contracts.[17,31,34] Benign lobulation is a result of hyperplasia of the adjacent connective tissue and cicatrical contraction.[12,17] In the present study, the malignancy rate was higher in lobulated GGNs than in GGNs without lobulation. The PPV was 93.5% (43/46); although 59.1% (39/66) of GGNs without lobulation were neoplastic. This finding is consistent with previous studies, which reported that lobulation was frequently indicative of malignancy.[19,35] Spiculation is induced by a desmoplastic response in the nodule, resulting in fibrotic strands radiating into the surrounding lung parenchyma.[27,36] As previously demonstrated, spiculation in GGNs is suggestive of neoplasms.[11,31,37] Our results showed that spiculation was an independent factor for the malignancy of GGNs. We found that 83.3% (50/60) of spiculated nodules were malignant, while 61.5% (32/52) of nodules without spiculation were malignant. Pleural tags mainly exist in lung adenocarcinomas with solid components. These tags are caused by a desmoplastic reaction of the solid component.[27,38] In the present study, 87.2% (34/39) of GGNs with pleural tags were neoplastic. Fan *et al*. and Murakami *et al*. also found significantly higher frequencies of the vascular convergence sign and pleural tags in malignant than in benign nodules.[39–40]

There are several limitations to the present study, which means that further investigation is required. First, the sample size of benign GGNs was small, especially for non-solid GGNs. Second, the evaluation of GGNs was subjective, which may result in selection bias. Third, because this was a retrospective study aimed at evaluating nodule characteristics on CT images and the advantage of 3D reconstruction to discriminate malignant from benign, pre-test risk factors were not taken into account. Finally, adenocarcinomas in Asians differ from those found in Caucasians.[41] Thus, epidemiologic and racial factors should be considered when interpreting our findings.

Conclusion

In conclusion, in GGNs, a solid component, vascular convergence sign, and a larger diameter are highly suggestive of neoplasms. Lobulation, spiculation, air cavity densities, and pleural tags are also signs of malignancy. Because benign nodules also manifest these characteristics, the qualitative diagnosis of GGNs should be carried out carefully. 3D nodule reconstruction is highly recommended as, from different angles, it can clearly and accurately display anatomical morphology and margin characteristics, enabling a comprehensive analysis of the nodules. Further research containing a larger sample size is needed to develop a more satisfactory method for the differential diagnosis of GGNs and an optimal surgery method. Bilateral and multiple GGNs should also be researched and carefully followed-up.

Disclosure

No authors report any conflict of interest.

References

1 Pastorino U. Current status of lung cancer screening. *Thorac Surg Clin* 2013; **23**: 129–40.
2 Korpanty G, Smyth E, Carney DN. Update on anti-angiogenic therapy in non-small cell lung cancer: Are we making progress? *J Thorac Dis* 2011; **3**: 19–29.
3 Chheang S, Brown K. Lung cancer staging: Clinical and radiologic perspectives. *Semin Interv Radiol* 2013; **30**: 99–113.
4 Huang Y, Wang YJ, Wang WY, Pu Q, Li WM. [Value of fGGO in diagnosing stage I lung cancers]. *Sichuan Da Xue Xue Bao Yi Xue Ban* 2014; **45**: 316–19. (In Chinese.)
5 Wahidi MM, Govert JA, Goudar RK *et al*. Evidence for the treatment of patients with pulmonary nodules: When is it lung cancer?: ACCP evidence-based clinical practice guidelines (2nd edition). *Chest* 2007; **132** (3 Suppl): 94s–107s.
6 Aberle DR, DeMello S, Berg CD *et al*. Results of the two incidence screenings in the National Lung Screening Trial. *N Engl J Med* 2013; **369**: 920–31.
7 Austin JH, Müller NL, Friedman PJ *et al*. Glossary of terms for CT of the lungs: Recommendations of the Nomenclature Committee of the Fleischner Society. *Radiology* 1996; **200**: 327–31.

8 Hansell DM, Bankier AA, MacMahon H, McLoud TC, Müller NL, Remy J. Fleischner Society: Glossary of terms for thoracic imaging. *Radiology* 2008; **246**: 697–722.
9 Theros EG. 1976 Caldwell Lecture: Varying manifestation of peripheral pulmonary neoplasms: A radiologic-pathologic correlative study. *AJR Am J Roentgenol* 1977; **128**: 893–914.
10 Li F, Sone S, Abe H, MacMahon H, Doi K. Malignant versus benign nodules at CT screening for lung cancer: Comparison of thin-section CT findings. *Radiology* 2004; **233**: 793–8.
11 Oh JY, Kwon SY, Yoon HI *et al*. Clinical significance of a solitary ground-glass opacity (GGO) lesion of the lung detected by chest CT. *Lung Cancer* 2007; **55**: 67–73.
12 Kim HY, Shim YM, Lee KS, Han J, Yi CA, Kim YK. Persistent pulmonary nodular ground-glass opacity at thin-section CT: Histopathologic comparisons. *Radiology* 2007; **245**: 267–75.
13 Beasley MB, Brambilla E, Travis WD. The 2004 World Health Organization classification of lung tumors. *Semin Roentgenol* 2005; **40**: 90–7.
14 Travis WD, Brambilla E, Noguchi M *et al*. International Association for the Study of Lung Cancer/American Thoracic Society/European Respiratory Society: International multidisciplinary classification of lung adenocarcinoma: Executive summary. *Proc Am Thorac Soc* 2011; **8**: 381–5.
15 Shi CZ, Zhao Q, Luo LP, He JX. Size of solitary pulmonary nodule was the risk factor of malignancy. *J Thorac Dis* 2014; **6**: 668–76.
16 Nakata M, Saeki H, Takata I *et al*. Focal ground-glass opacity detected by low-dose helical CT. *Chest* 2002; **121**: 1464–7.
17 Ost D, Fein AM, Feinsilver SH. Clinical practice. The solitary pulmonary nodule. *N Engl J Med* 2003; **348**: 2535–42.
18 Naidich DP, Bankier AA, MacMahon H *et al*. Recommendations for the management of subsolid pulmonary nodules detected at CT: A statement from the Fleischner Society. *Radiology* 2013; **266**: 304–17.
19 Li Y, Chen KZ, Wang J. Development and validation of a clinical prediction model to estimate the probability of malignancy in solitary pulmonary nodules in Chinese people. *Clin Lung Cancer* 2011; **12**: 313–19.
20 Henschke CI, McCauley DI, Yankelevitz DF *et al*. Early Lung Cancer Action Project: Overall design and findings from baseline screening. *Lancet* 1999; **354**: 99–105.
21 Nakazono T, Sakao Y, Yamaguchi K, Imai S, Kumazoe H, Kudo S. Subtypes of peripheral adenocarcinoma of the lung: Differentiation by thin-section CT. *Eur Radiol* 2005; **15**: 1563–8.
22 Henschke CI, Yankelevitz DF, Mirtcheva R *et al*. CT screening for lung cancer: Frequency and significance of part-solid and nonsolid nodules. *AJR Am J Roentgenol* 2002; **178**: 1053–7.
23 Folkman J. What is the evidence that tumors are angiogenesis dependent? *J Natl Cancer Inst* 1990; **82**: 4–6.
24 Birau A, Ceausu RA, Cimpean AM, Gaje P, Raica M, Olariu T. Assessement of angiogenesis reveals blood vessel heterogeneity in lung carcinoma. *Oncol Lett* 2012; **4**: 1183–6.
25 Parera MC, van Dooren M, van Kempen M *et al*. Distal angiogenesis: A new concept for lung vascular morphogenesis. *Am J Physiol Lung Cell Mol Physiol* 2005; **288**: L141–149.
26 Mori K, Saitou Y, Tominaga K *et al*. Small nodular lesions in the lung periphery: New approach to diagnosis with CT. *Radiology* 1990; **177**: 843–9.
27 Kuriyama K, Tateishi R, Doi O *et al*. CT-pathologic correlation in small peripheral lung cancers. *AJR Am J Roentgenol* 1987; **149**: 1139–43.
28 Gaeta M, Caruso R, Blandino A, Bartiromo G, Scribano E, Pandolfo I. Radiolucencies and cavitation in bronchioloalveolar carcinoma: CT-pathologic correlation. *Eur Radiol* 1999; **9**: 55–9.
29 Kuriyama K, Tateishi R, Doi O *et al*. Prevalence of air bronchograms in small peripheral carcinomas of the lung on thin-section CT: Comparison with benign tumors. *AJR Am J Roentgenol* 1991; **156**: 921–4.
30 Farooqi AO, Cham M, Zhang L *et al*. Lung cancer associated with cystic airspaces. *AJR Am J Roentgenol* 2012; **199**: 781–6.
31 Nambu A, Araki T, Taguchi Y *et al*. Focal area of ground-glass opacity and ground-glass opacity predominance on thin-section CT: Discrimination between neoplastic and non-neoplastic lesions. *Clin Radiol* 2005; **60**: 1006–17.
32 Kohno N, Ikezoe J, Johkoh T *et al*. Focal organizing pneumonia: CT appearance. *Radiology* 1993; **189**: 119–23.
33 Patel VK, Naik SK, Naidich DP *et al*. A practical algorithmic approach to the diagnosis and management of solitary pulmonary nodules: Part 1: Radiologic characteristics and imaging modalities. *Chest* 2013; **143**: 825–39.
34 Nakajima R, Yokose T, Kakinuma R, Nagai K, Nishiwaki Y, Ochiai A. Localized pure ground-glass opacity on high-resolution CT: Histologic characteristics. *J Comput Assist Tomogr* 2002; **26**: 323–9.
35 Zerhouni EA, Stitik FP, Siegelman SS *et al*. CT of the pulmonary nodule: A cooperative study. *Radiology* 1986; **160**: 319–27.
36 Zwirewich CV, Vedal S, Miller RR, Müller NL. Solitary pulmonary nodule: High-resolution CT and radiologic-pathologic correlation. *Radiology* 1991; **179**: 469–76.
37 Lee KS, Yi CA, Jeong SY *et al*. Solid or partly solid solitary pulmonary nodules: Their characterization using contrast wash-in and morphologic features at helical CT. *Chest* 2007; **131**: 1516–25.
38 Winer-Muram HT. The solitary pulmonary nodule. *Radiology* 2006; **239**: 34–49.
39 Fan L, Liu SY, Li QC, Yu H, Xiao XS. Multidetector CT features of pulmonary focal ground-glass opacity: Differences between benign and malignant. *Br J Radiol* 2012; **85**: 897–904.
40 Murakami T, Yasuhara Y, Yoshioka S, Uemura M, Mochizuki T, Ikezoe J. Pulmonary lesions detected in population-based CT screening for lung cancer: Reliable findings of benign lesions. *Radiat Med* 2004; **22**: 287–95.
41 Gao B, Sun Y, Zhang J *et al*. Spectrum of LKB1, EGFR, and KRAS mutations in Chinese lung adenocarcinomas. *J Thorac Oncol* 2010; **5**: 1130–5.

